IJPSR (2019), Volume 10, Issue 12 **(Research Article)**

INTERNATIONAL JOURNAL OF PHARMACEUTICAL SCIENCES AND RESEARCH

Received on 22 August 2019; received in revised form, 16 November 2019; accepted, 26 November 2019; published 01 December 2019

STUDY OF MANGIFERIN ISOLATED FROM LEAVES OF *MANGIFERA INDICA* ON MYELOID LEUKEMIA ALONG WITH DIFFERENT HUMAN CANCER CELL LINES

Hemanth Kumar Manikyam

Faculty of Science, Department of Chemistry, North East Frontier Technical University, Aalo - 791001, Arunachal Pradesh, India.

Keywords:

Tyrosine Kinase, Mangiferin, Ayurveda Shastra, Indian Traditional Medicine (ITM), Leukaemia

Correspondence to Author:
Hemanth Kumar Manikyam

Faculty of Science, Department of Chemistry, North East Frontier Technical University, Aalo - 791001, Arunachal Pradesh, India.

E-mail: phytochem2@gmail.com

ABSTRACT: In different myeloid leukemia cases resistance to diverse treatment regimen owes to multiple molecular mechanisms of cellular network. Epigenetic dysregulation, gene mutations, overexpression of multidrug resistance genes, abnormal immune function, the presence of chemotherapy-resistant leukemia-initiating cells, and aberrant signaling pathways could be the lead cause of this kind of aberration. Some marketed drug is considered as a first-generation drug that can inhibit the enzymatic action by inhibiting the ATP binding with different key pathway regulator protein. Later on, insensitivity of myeloid leukemia cells towards these drugs has been observed may be due to mutation in tyrosine kinase domain of the kinase receptor. By enchanting into account of bioavailability and resistance developed, there is an extreme need to find some natural and nature-derived inhibitors for the kinase proteins of different key metabolic pathways. For computational screening and *in-vitro* studies against cancer cell lines and marker proteins, Mangiferin and Euxanthic acid isolated from leaves of *Mangifera indiaca* had been used as mentioned in Ayurveda / Indian Traditional Medicine (ITM). Docking analysis was also carried out on the active site of different tyrosine kinase receptors with reported reference inhibitors. A series of *in-vitro* tests were done to validate the stability of the system. The anti-proliferative effect of Mangiferin as tested and was found to inducing cell death with IC_{50} values 149 µg/ml in K-562 and 297 µg/ml in Jurkat cells respectively. Considering the above-said parameters proposed Mangiferin molecule is concluded as potential lead for drug designing pipeline against myeloid leukemia.

INTRODUCTION: In 2014, approximately 18 000 adults were identified with acute myeloid leukemia (AML) in the United States of America [1]. The backbone rehabilitation procedure of AML is the combination of cytarabine and an anthracycline. This regimen was initially established about 4 decades ago and remained the standard of care [2].

QUICK RESPONSE CODE

DOI: 10.13040/IJPSR.0975-8232.10(12).5545-52

The article can be accessed online on www.ijpsr.com

DOI link: http://dx.doi.org/10.13040/IJPSR.0975-8232.10(12).5545-52

In spite of substantial improvements in decoding AML, the bulk of patients died from their disease. In the previous 30 odd years overall survival rate of seniors (median age 66 years) has not altered, and the cure rates less than 10% while median survival less than 1 year [3-5].

Although about 80% of patients below 60 years of age can get complete reductions, most eventually relapse and 5-year survival is only 40-50% in that age group [5-7]. Therefore, the need for new treatment strategies for AML is evident. Multiple molecular mechanisms contribute to resistance in the treatment regimen in a diverse AML. Epigenetic dysregulation, gene mutations, overexpression of

multidrug resistance genes, abnormalmimmune function, the presence of chemotherapy-resistant leukemia-initiating cells, and aberrant signaling pathways *(i.e.*, phosphatidylinositol 3-kinase / protein kinase B (PI3K/ AKT) mammalian target of rapamycin (mTOR) and Wnt could be the lead cause of it [5]. The revolutionary treatment for leukemia came into reality after the discovery of Imatinib [16]. Imatinib, a Type-II tyrosine kinase inhibitor, which mainly inhibits the cancerous cell division and less affects the normal cells [17, 18]. Type-II inhibitors can inhibit the target in its inactive stage and fixes to the hydrophobic pocket which is head-to-head to the ATP binding site [17, 22]. When Imatinib blocked the ATP binding site of Tyrosine Kinases it cascaded into subsequent blockage of signaling process. One of the major restrictions of Imatinib is that it is mainly effective in initial phases but slightest active in case of late-onset of myeloid leukemia [17, 23, 24]. There are some cases reports which indicate that after treatment with Imatinib reoccurrence of cancer in freshly treated and advanced staged patients [25]. BCR-ABL tyrosine kinase protein inhibitions have been shown by some second-generation inhibitor drugs like Baustinib, Tozaseritib, Nilotinib and Befatinib [26]. Due to restrictions of binding capacity and bioavailability of the above-said inhibitors, holistic metabolic pathway target-based therapy for the myeloid leukemia is highly needed [27].

In work to discover new potent effective treatment of myeloid leukemia, we studied natural and nature-derived agents including Mangeferin and Euxanthic Acid. Naturally acquired compounds are deliberated as safer as well as biodegradable than synthetic and semi-synthetic compounds. The problem of drug resistance observed in synthetic and semi-synthetic drugs is also reduced [6]. Plants epitomize a cradle of numerous pharmaceutically important phytochemical compounds. The secondary metabolites present in plants have been used in handling a number of human diseases. Mostly drugs and drug-like molecules are obtained from medicinal plants. 25% of total drugs in developed and 85% in developing countries are obtained from natural resources [7]. These drugs have various modes of action, their combination is more likely superior to single-agent with respect to potentially targeting different pathways in cancer cells, overcoming drug resistance and maximizing therapeutic efficacy. Mangiferin is a xanthanoid. This is a glucoside of norathyriol. It's originated in mangoes, [8] in iris unguicularis [9], anemarrhena asphodeloides rhizomes [10] and in *Bombax ceiba* [11]. It can be found in the genera Salacia and Cyclopia. [12] laboratory studies have identified a variety of potential pharmacological attributes encompassing anti-microbial and anti-oxidant activities [13] inhibitory effects of type II 5α- reductase *in-vitro* [14] and gastroprotective [15] and anti-diabetic [10] effects in rodents.

MATERIALS AND METHODS:

Ensemble Docking Protocol:

Receptor Preparation: From the substantial pool of the Crystal structures of various tyrosine kinase accessible in the protein databank, the structures with goals with under 2.5 Å, with co-crystal inhibitors, without breaks in the coupling site were chosen for encouraging investigation. Every one of the structures was superimposed to comprehend the adaptability of the coupling site. In view of the adaptability of the coupling site four co-crystal structures *viz.* 4DRH, 4WAF, 4WOY, and 3QKM were chosen from the Protein Data Bank (PDB). Four Crystal structures of mTOR, PI3K, DRP1, and AkT tyrosine kinase structures were pre-handled utilizing the protein readiness to dole out bond arranges and refine the structure including hydrogen bond advancement and obliged minimization [28]. Where required, missing side chains were included utilizing Prime [29, 30]. For each protein structure one chain alongside its ligand was kept and water particles were erased past 5 Å from heteroatom gatherings. What's more, the interior hydrogen bond arrange was upgraded, trailed by compelled vitality minimization.

Docking Protocol: For the three streamlined protein structures lattices based possibilities were created for the coupling destinations utilizing Glide Grid Generation with default settings alongside the rotatable bond settings for the OH and SH gatherings of the coupling site amino acids. Mixes acquired by means of Lig-Prep for all mixes were docked against the readied three Crystal structures of neuraminidase proteins utilizing Glide additional exactness (XP) with the default settings [33-35]. The docking scores were broke down with the default XP-present watcher record. In view of model assessment results best pose for the best ligand

portrayal was made. Re-docking of every co-crystal ligand into its relating structure dynamic site approved our docking setup to produce models; for each situation the co-gem present was replicated with RMSD esteems <1.5 A0. Assist assessment of the docking model cross-docking of the ligands to other neuraminidase proteins structures in the nearness and non-appearance of water.

Test System Preparation: Prior to the assay the test system A549, HepG2, K562, Jurkat and MCF-7 cells were propagated at 37 ± 1 °C in a gaseous environment of 5% ± 1% Carbon dioxide, in humid environment in tissue culture flasks containing medium, Dulbecco's Modified Eagle Medium (DMEM) (Invitrogen, USA) supplemented with 10% fetal bovine serum (Invitrogen, USA) and penicillin (100 units) – streptomycin (100 µg) antibiotics (Invitrogen, USA) to obtain the sub confluence of cells (70% to 90% Confluent).

Cell Seeding for Cytotoxicity Assessment: Cell monolayer was rinsed with PBS, aspirated off PBS and cells were trypsinized with 0.25% Trypsin with 0.2 g/l EDTA in tissue culture flask at 37 ± 1 °C until the cells detached and floated. DMEM with 10% FBS was added into the flask to flush out the cells and centrifuged at 900 rpm for 5 min. Cells were re-suspended in DMEM medium, and the cell suspension was subjected for the cell count and viability to determine cell number per ml. Cell number was adjusted to 2×10^5 cells/ml, and 0.1 ml of the adjusted cells were seeded in each well of 96 well cell culture plates. Frequent mixing was done during the seeding, to achieve a uniform cell suspension for plating the cells per well. Plates were designated to indicate its contents and date of experiment. Plates were incubated at 37 ± 1 °C for 24 ± 1 h in gaseous environment of 5% ± 1% Carbon dioxide.

From the final stock different concentrations of the final working stocks, five concentrations were prepared in DMEM medium by 4 folds and 3 folds serial dilutions as specified in table below. Diluted stocks were used for the study.

Treatment: After 24 ± 1 h incubation the cell was exposed to different concentrations of test items **Table 3** by replacing the spent medium with 100 µl of different concentrations of the test items solution and incubated for 48 ± 1 h at 37 ± 1 °C in gaseous environment of 5 ± 1% carbon dioxide. Positive, negative control and blank were dispensed in the designated wells and incubated for 48 ±1 hours at 37 ± 1 °C in gaseous environment of 5 ± 1% carbon dioxide. At the end of the 48 ± 1 h incubation medium with test item / positive control was removed, and cells were incubated for 4 h with 20 µl of MTT 5 mg/ml solution. After 4 h incubation formazan crystals formed by mitochondrial reduction of MTT was solubilized by adding 150 µl of DMSO. Absorbance was read at 570 nm after 10 min incubation with vortexing.

Annexin V and Propidium Iodide Assay Principle: Annexins are a family of calcium-dependent phospholipid-binding proteins that preferentially bind phosphatidylserine (PS). Under normal physiologic conditions, PS is predominantly located in the inner leaflet of the plasma membrane. Upon initiation of apoptosis, PS loses its asymmetric distribution across the phospholipid bilayer and is translocated to the extracellular membrane leaflet marking cells as targets of phagocytosis.

Once on the outer surface of the membrane, PS can be detected by fluorescently labeled Annexin V in a calcium-dependent manner. In early-stage apoptosis, the plasma membrane excludes viability dyes such as propidium iodide (PI).

These cells will stain with Annexin V but not a viability dye, thus distinguishing cells in early apoptosis. However, in late-stage apoptosis, the cell membrane loses integrity thereby allowing Annexin V to also access PS in the interior of the cell. A viability dye can be used to resolve these late-stage apoptotic and necrotic cells (Annexin V, viability dye-positive) from the early-stage apoptotic cells (Annexin V positive, viability dye negative)

Cell Apoptosis Staining Assay Procedure: Dilute 10X Binding Buffer to 1X using distilled water (1 mL 10X Binding Buffer + 9 mL dH20). Harvest cells. Wash cells once in 1X PBS, then once in 1X Binding Buffer. Resuspend cells in 1X Binding Buffer at 1-5 × 10^6 cells/mL. Add 5 µL of fluorochrome-conjugated Annexin V to 100 µL of

the cell suspension. Incubate 10-15 min at room temperature, protected from light. Wash cells with 2 mL 1X Binding Buffer and resuspend in 200 µL of 1X Binding Buffer. Add 5 µL of Propidium Iodide Staining Solution or 7-AAD Viability Staining Solution. Analyze by flow cytometry within 4 h, storing at 2-8 ºC in the dark.

Data Analysis: A decrease in the number of living cells results in a decrease in metabolic activity in the sample. This decrease directly correlates to the amount of formazan formed as monitored by optical density at 570 nm. Percent Viability will be calculated using the below formula [19, 20, 21].

% Viability = 100 (O. D. Test Item / O. D. of Control)

% Activity = 100 - % Viability

RESULTS AND DISCUSSION:

Examination of Target Atoms Against Various Tyrosine Kinase: A dataset of little atoms that involves 1000 regular mixes of the ITM database have been utilized for the virtual screening of mTor (4DRH), PI3k (4WAF), DRP1 (4WOY) and AkT (3QKM). A cut-off scope of docking score had been set as - 6.00 kcal/mol, which is higher than all accessible reference particles. Top ligand particles, whose docking score was higher than - 6.00 kcal/mol were chosen for advance examination. All cooperating atoms with docking score, number of H-bond and side chain, collaborating build-ups and some different associations are recorded in **Fig. 1**. Ligands are positioned based on their docking scores. Protein-Ligand associations appear in **Fig. 1**, as protein-ligand interaction outline.

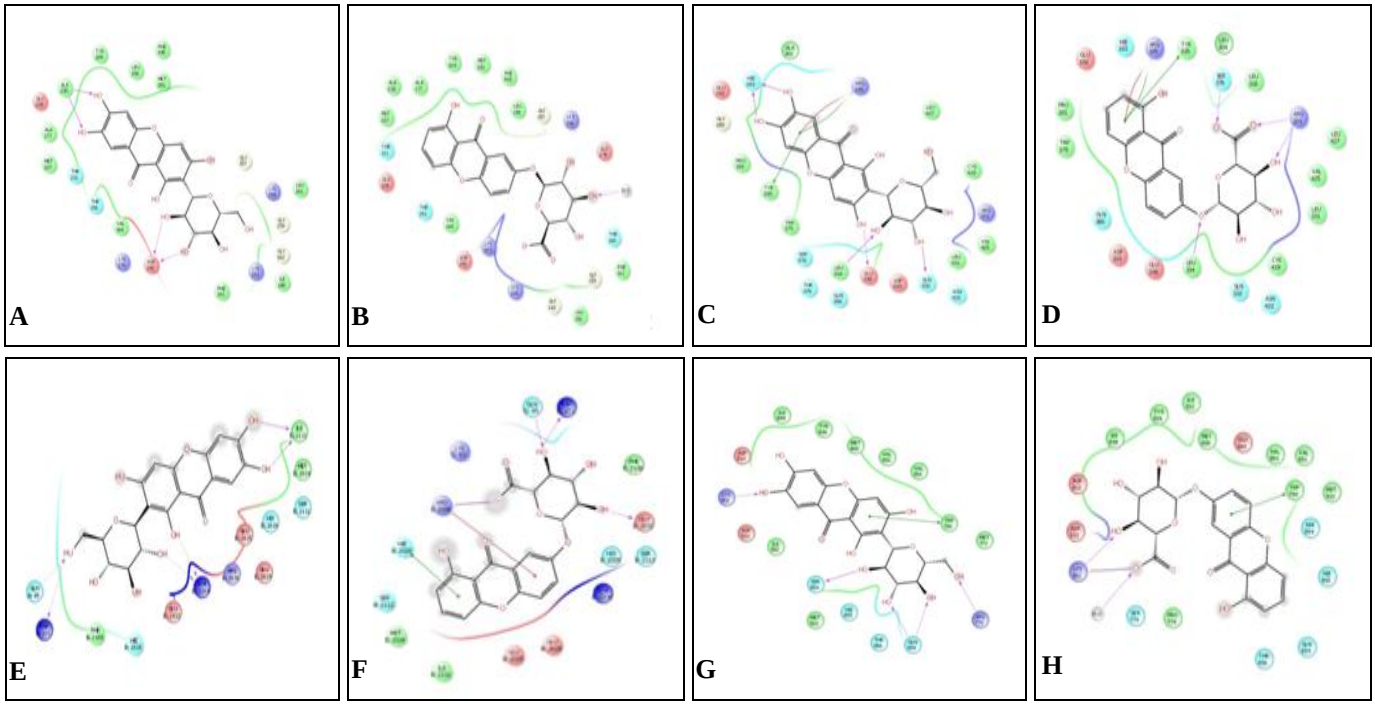

FIG. 1: EXAMINATION OF TARGET ATOMS AGAINST VARIOUS TYROSINE KINASE Akt: A Mangiferin: Backbone hydrogen bonding with Ala 210, Sidechain hydrogen is bonding with Asp 292. B. Euxanthic acid: No prominent Hydrogen bonding with receptor molecule but intrinsic H2O molecule contributes to molecule stabilization. Vander Wall interaction shown by Phe 436, Met 281, Tyr 229, Ala177, Ala 230, Met 227, Thr 211, Glu 228, Thr 291, Val 164, Asp 292, Lys 163, Lys 179, Gly 162, Leu 181, Gly 199, Phe 161, Thr 160, Glu 278, Lys 158, Gly 157, Leu 156. DRP1: C Mangiferin: Backbone hydrogen bonding with His 193, Leu 334, Gln 332, Sidechain hydrogen bonding with Glu 338.Pose and stereospecific Pi-Pi bond formed with Arg 195 and Tyr 335. Arg 195 also shown Pi-Cataion bond. D: Euxanthic Acid: Backbone hydrogen bonding with Leu 334, Sidechain hydrogen bonding with Glu 338, Arg 221, Ser 376.Pose and stereospecific Pi-Pi bond formed with Arg 195 and Tyr 335. Arg 195 also shown Pi-Cataion bond. mTOR: E Mangiferin: Backbone hydrogen bonding with E chain ILeu 2111, Sidechain hydrogen bonding with A chain Gln 85, RAP 201, B chain co-crystal mol SO4 2204. F Euxanthic acid: Sidechain hydrogen bonding with D chain Gln 85, RAP 201, E chain Glu 2112. E chain Arg 2036 shown Pi cation bond along with positive negative electrostatic bond. A pose and stereospecific bond formed with B chain His 2028. PI3K: G Mangiferin: Backbone hydrogen bonding with Ser 854, Sidechain hydrogen is bonding with Lys 802, Arg 770, Gln 859. Pose and stereospecific Pi-Pi bond formed with Trp 780. HEuxanthic acid: Sidechain hydrogen bonding with Lys 802 and IntrinsicH2O molecule along with positive - negative electrostatic bond with Lys 802.Pose and stereospecific Pi-Pi bond formed with Trp 780.

Interaction Study of the Complex: Mangiferin particle indicated interaction with hydrogen bonding at Ala 210 and with side-chain hydrogen bonding at Asp 292 with AkT while DRP1 demonstrated interaction by means of hydrogen bonding with His 193, Leu 334, Gln 332 and side-chain hydrogen bonding with Glu 338. An extremely pose and stereo particular Pi-Pi bond shaped with Arg 195 and Tyr 335 and Arg 195 demonstrated Pi-Cataion security with DRP1 by mangiferin. PI3K restricting pocket bound with mangiferinwith hydrogen bonding at Ser 854 and side-chain hydrogen bonding with Lys 802, Arg 770, Gln 859.

It additionally demonstrated Pose and stereo particular Pi-Pi security framed with Trp 780 while mTOR protein just indicated hydrogen bonding with E chain ILeu 2111 and side-chain hydrogen bonding with A chain Gln 85, RAP 201, B chain co-crystal mol SO4 2204. Akt protein structure interfaced with Euxanthic corrosive with no noticeable hydrogen bonding however inborn H_2O particle contributes to atom adjustment. Vander Wall interaction appeared by Phe 436, Met 281, Tyr 229, Ala177, Ala 230, Met 227, Thr 211, Glu 228, Thr 291, Val 164, Asp 292, Lys 163, Lys 179, Gly 162, Leu 181, Gly 199, Phe 161, Thr 160, Glu 278, Lys 158, Gly 157, Leu 156. If there should be an occurrence of DRP1 structure and Euxanthic Acid interaction it indicated hydrogen bonding with Leu 334 and side-chain hydrogen bonding with Glu 338, Arg 221, Ser 376. An extremely pose and stereo particular Pi-Pi bond shaped with Arg 195 and Tyr 335 and Arg 195 indicated Pi-Cataion bond.

mTOR protein and Euxanthic corrosive communicated at side-chain hydrogen bonding with D chain Gln 85, RAP 201, E chain Glu 2112. E chain Arg 2036 while additionally indicated Pi cation bond alongside positive negative electrostatic bond. A pose and stereo particular bond shaped with B chain His 2028 Euxanthic corrosive indicated interaction with PI3K protein side-chain hydrogen bonding with Lys 802 and Intrinsic H_2O particle alongside positive – negative electrostatic bond with Lys 802. An extremely pose and stereo particular Pi-Pi bond additionally shaped with Trp 780. These two-atom interaction points of interest were appeared in **Table 1**, **Fig. 2**.

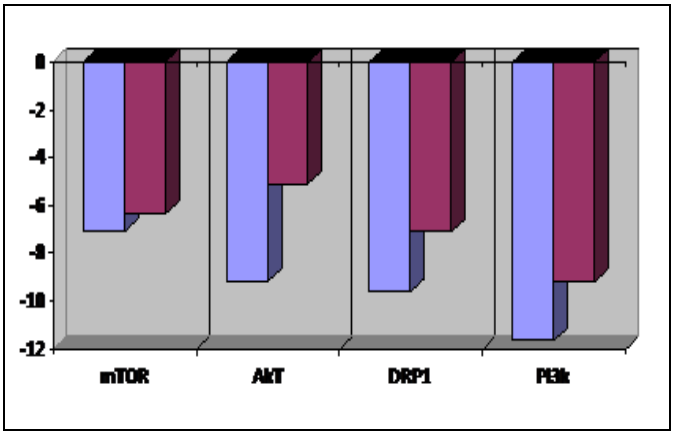

FIG. 2: IT SHOWS THAT DIFFERENT KEY METABOLIC PATHWAY REGULATOR TYROSINE KINASES CAN BE INHIBITED BYMANGEFIRIN (BLUE) AND EUXANTHIC ACID (MAGENDA) MOLECULE. MANGEFERIN ACTS AS BETTER INHIBITOR OVER EUXANTHIC ACID IN ALL THE TYROSINE KINASES

MTT Assay: All the cells were harvested from the culture and seeded in the 96 well assay plates at a seeding density of 2.0×10^4 cells/well and were incubated for 24 h. Test item Mangiferin were exposed at the concentrations of 1.25, 0.313, 0.078, 0.02, 0.005 and 0.001 mg/ml, respectively and incubated for a period of 48 h followed by dispensing MTT solution (5 mg/ml). The cells were incubated at 37 ± 1 °C for 4 h followed by addition of DMSO for dissolving the formazan crystals and absorbance was read at 570 nm. Separate wells were prepared for positive control, controls (only medium with cells), and blank (only medium). Percent viability and activity was calculated at different concentrations.

Anticancer Activity on Different human Cancer Cell lines:

Anticancer Activity on A549 Cells: Mangiferin was found to have an inhibition activity of 88% at a concentration of 1.25 µg/ml. Positive controls Doxorubicin and Mitomycin C were found to have inhibition activity of 93% and 87% respectively at a concentration of 100 µg/ml.

Anticancer Activity on Hep-G2 Cells: Mangiferin was found to have an inhibition activity of 100% at a concentration of 1.25 µg/ml. Positive controls Doxorubicin and Mitomycin C were found to have inhibition activity of 107% and 100% respectively at a concentration of 100 µg/ml.

Anticancer Activity on MCF-7 Cells: Mangiferin was found to have an inhibition activity of 97% at a

concentration of 1.25 µg/ml. Positive controls Doxorubicin and Mitomycin C were found to have inhibition activity of 76% and 100% respectively at a concentration of 100 µg/ml.

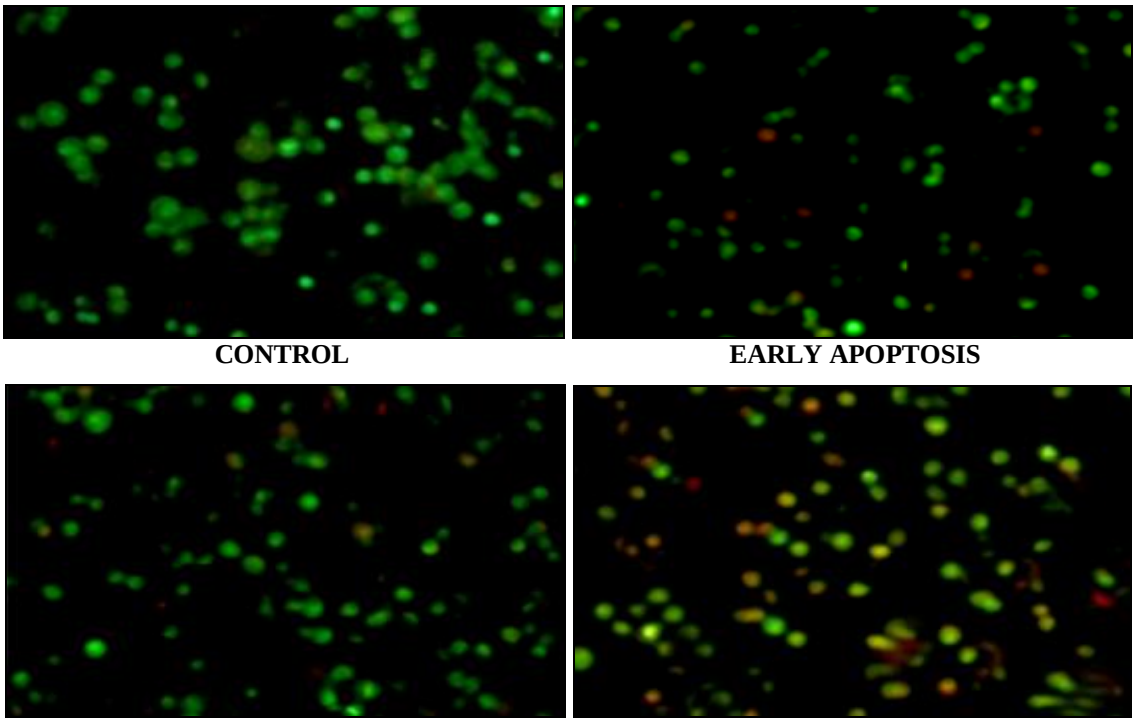

FIG. 3: CELLS TREATED WITH ANNEXIN AND PROPIDIUM IODIDE TO DETERMINE MANGIFERIN INDUCING APOPTOSIS RATHER THAN NECROSIS

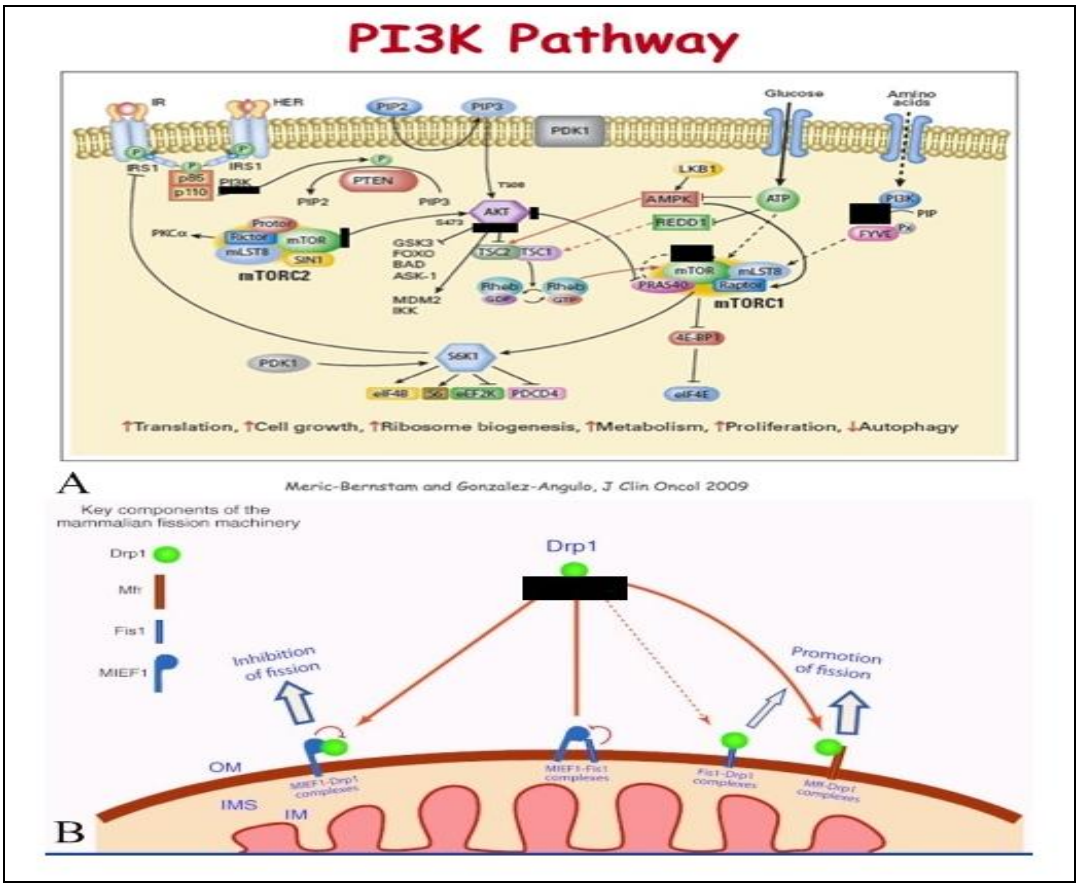

FIG. 4: PROPOSED PATHWAYS FOR MANGIFERIN ACTIVITY ON DIFFERENT CANCER PATHWAYS. BLACK COLORED BOX IN PICTURES INDICATE THE INHIBITION OF THE PARTICULAR PROTEIN IN THE CANCER PATHWAY

Anticancer Activity on Jurkat Cells: Mangiferin was found to have an inhibition activity of 100% at a concentration of 1.25 µg/ml. Positive controls Doxorubicin and Mitomycin C were found to have inhibition activity of 99% and 95% respectively at a concentration of 100 µg/ml.

Anticancer Activity on K-562 Cells: Mangiferin was found to have an inhibition activity of 94% at a concentration of 1.25 µg/ml.

CONCLUSION: Tyrosine kinase domain inhibition of these proteins complex targeted by rational drug designing is quite an attractive approach to treat myeloid leukemia patients. In this study, inhibitors for key proteins of different metabolic pathways have been proposed as successor of the known inhibitors for effective treatment of CML through virtual screening and cell line-based essay test. Mangiferin and Euxanthic acid molecules were selected on the basis of their high docking score. Highest scoring compound Mangiferin with protein complex was chosen over Euxanthic acid for different tyrosine-based kinases in different metabolic pathways. Mangiferin forms hydrogen bond with Ser 854 backbone and side-chain hydrogen bonding with Lys 802, Arg 770, Gln 859. Pose and stereospecific Pi-Pi bond formed with Trp 780.

The anti-proliferative effect of Mangiferin as tested and was found to inducing cell death with IC-50 values 149 µg/ml in K-562 and 297 µg/ml in Jurkat cells respectively. Due to the low bioavailability of Mangiferin efficacy of it may get affected. Many studies have proved combination of Mangiferin with lipids increase its bioavailability many folds [36]. Lipo based encapsulation technology may prove more effective in drug delivery system of Mangiferin. We may conclude that Mangiferin may acts as potential drug candidate for the treatment of Myeloid Leukemia by inhibiting different metabolic pathways *viz* PI3K, mTOR, *etc.*, although other experimental aspects also need to be taken care of it. We propose a hypothetical blockage of key metabolic pathways of leukemia, by a schematic representation **Fig. 4**.

ACKNOWLEDGEMENT: We thank Imperial Life Sciences for providing the opportunity to undertake this research, and we thank the Schrodinger software team for providing critical input for this research.

CONFLICTS OF INTEREST: Nil

REFERENCES:

1. Siegel R, De Santis C and Jemal A: Colorectal cancer statistics. CA: a Cancer J for Clin 2014; 64(2): 104-17.
2. Yates JW, Wallace Jr, HJ, Ellison RR and Holland JF: Cytosine arabinoside (NSC-63878) and daunorubicin (NSC-83142) therapy in acute nonlymphocytic leukemia. Cancer Chemotherapy Reports 1973; 57(4): 485.
3. Burnett AK, Hills RK, Milligan DW, Crystal GAH, Prentice AG, McMullin MF and Wheatley K: Attempts to optimize induction and consolidation treatment in acute myeloid leukemia: results of the MRC AML12 trial. Journal of Clinical Oncology 2010; 28(4): 586-95.
4. Büchner T, Berdel WE, Haferlach C, Haferlach T, Schnittger S, Müller-Tidow C, Braess J, Spiekermann K, Kienast J, Staib P, Grüneisen A, Kern W, Reichle A, Maschmeyer G, Aul C, Lengfelder E, Sauerland MC, Heinecke A, Wörmann B, Hiddemann W and ClinOncol J: Age-related risk profile and chemotherapy dose-response in acute myeloid leukemia: a study by the German Acute Myeloid Leukemia Cooperative Group 2009; 27(1): 61-9.
5. Roboz GJ: Current treatment of acute myeloid leukemia. Current Opinion in Oncology 2012; 24(6): 711-19.
6. Kumar MH, Dhiman V, Choudhary R and Chikara A: Anticancer activity of hydroalcoholic extracts from Paris polyphylla rhizomes against human A549 lung cancer cell lines using MTT assay. International Research Journal of Pharmacy 2014; 5(4): 290-94.
7. Tiwari JK, Ballabha R and Tiwari P: Ethnopaediatrics in Garhwal Himalaya, Uttarakhand, India (Psychomedicine and Medicine). New York Science J 2010; 3(4): 123-26.
8. Barreto JC, Trevisan MTS, Hull WE, Erben G, De Brito ES, Pfundstein B, Würtele G, Spiegelhalder B and Owen RW: Characterization and quantitation of polyphenolic compounds in bark, kernel, leaves and peel of mango (*Mangifera indica* L.). Journal of Agricultural and Food Chemistry 2008; 56(14): 5599-10.
9. Atta-Ur-Rahman, Hareem, Sumaira, Choudhary I, Sener M, Abbaskhan B, Siddiqui A, Anjum H, Orhan S, Gurbuz I, Ayanoglu I and Filiz: New and Known Constituents from Iris unguicularis and Their Anti-oxidant Activity. Heterocycles 2010; 82: 813.
10. Miura T, Ichiki H, Hashimoto I, Iwamoto N, Kato M, Kubo M, Ishihara E, Komatsu Y, Okada M, Ishida T and Tanigawa K: Anti-diabetic activity of a xanthone compound, mangiferin. Phyto 2001; 8(2): 85-87.
11. Dar A, Faizi S, Naqvi S, Roome T, Zikr-Ur-Rehman S, Ali M, Firdous S and Moin ST: Analgesic and antioxidant activity of mangiferin and its derivatives: The structure activity relationship. Biological and Pharmaceutical Bulletin 2005; 28(4): 596-00.
12. Smith, Dale M, Harborne and Jeffrey B: Xanthones in the Appalachian Asplenium complex. Phyto 1971; 10 (9): 2117-19
13. Stoilova I, Gargova S, Stoyanova A and Ho L: Anti-microbial and anti-oxidant activity of the polyphenol mangiferin. Herba Polonica 2005; 51(1/2): 37–44.
14. Wang, X, Liao J, Yin D, Zhan F, Dai S, Xie G and Sang X: Establishment of a Novel Model for Studying the Effects of Extracts of Chinese Herb Medicine on Human

Type II 5-alpha-Reductase *in-vitro*. Yakugaku Zasshi 2010; 130(9): 1207-14.
15. Carvalho A, Guedes M, De Souza A, Trevisan M, Lima A, Santos FV and Rao V: Gastroprotective Effect of Mangiferin, a xanthonoid from *Mangifera indica*, against gastric injury induced by ethanol and indomethacin in rodents. Planta Medica 2007; 73(13): 1372-76.
16. Pray L: Gleevec: the breakthrough in cancer treatment. Nature Education 2008; 1(1): 37.
17. Savage DG and Antman KH: Imatinib mesylate-a new oral targeted therapy. New Eng J of Med 2002; 346(9): 683-93.
18. An X, Tiwari AK, Sun Y, Ding PR, Ashby CR and Chen ZS: 2010 BCR-ABL tyrosine kinase inhibitors in the treatment of Philadelphia chromosome-positive chronic myeloid leukemia: a review. Leukemia Research 2010; 34(10): 1255-68.
19. Kumar MH, Dhiman V, Choudhary R and Chikara A: Anti-cancer activity of hydroalcoholic extracts from Paris polyphylla rhizomes against human A549 lung cancer cell lines using MTT assay. International Research Journal of Pharmacy 2014; 5(4): 290-94.
20. Balakrishna A and Kumar MH: Evaluation of synergetic anticancer activity of berberine and curcumin on different models of A549, Hep-G2, MCF-7, Jurkat and K562 cell lines. Bio Med Research International 2015.
21. Kumar MH and Ramesh C: Anti-cancer activity of nano encapsulated formulation from the extracts of *Picrorhiza kurroa* against human cancer cell lines. Journal of Pharmacognosy and Phytochemistry 2014; 2(5): 135-38.
22. Druker BJ: Imatinib as a paradigm of targeted therapies. Advances in Cancer Research 2004; 91: 1-30.
23. Sherbenou and Daniel W: BCR-ABL SH3-SH2 domain mutations in chronic myeloid leukemia patients on imatinib. Blood 2010; 116(17): 3278-85.
24. Deininger and Michael WN: The tyrosine kinase inhibitor CGP57148B selectively inhibits the growth of BCR-ABL–positive cells. Blood (1997); 90(9): 3691-98.
25. Gorre and Mercedes E: Clinical resistance to STI-571 cancer therapy caused by BCR-ABL gene mutation or amplification. Science (2001); 293(5531): 876-80.
26. Heinrich and Michael C: Inhibition of c-kit receptor tyrosine kinase activity by STI 571, a selective tyrosine kinase inhibitor. Blood 2000; 96(3): 925-32.
27. Demetri GD: Phase 3, multicenter, randomized, double-blind, placebo-controlled trial of SU11248 in patients (pts) following failure of imatinib for metastatic GIST. ASCO Annual Meeting Proceedings. Supp 2005; 23(16).
28. Friesner: Extra Precision Glide: Docking and scoring incorporating a model of hydrophobic enclosure for protein-ligand complexes. J Med Chem 2006; 49: 6177-96.
29. Halgren TA: Glide: a new approach for rapid, accurate docking and scoring 2 enrichment factors in database screening. J Med Chem 2004; 47: 1750-759.
30. Friesner RA: Glide: a new approach for rapid, accurate docking and scoring. 1. method and assessment of docking accuracy. ournal of Medicinal Chemistry 2004; 47: 1739-49.
31. Hariharan R: Multimcs: a fast algorithm for the maximum common substructure problem on multiple molecules. Journal of Chemical Information and Modeling 2011; 51: 788-06.
32. Shivakumar D: prediction of absolute solvation free energies using molecular dynamics free energy perturbation and the OPLS force field. Journal of Chemical Theory and Computation 2010; 6: 1509-19.
33. Guo Z: Probing the α-helical structural stability of stapled p53 peptides: molecular dynamics simulations and analysis. Chem Biol Drug Des 2010; 75: 348-59.
34. Bowers KJ: Scalable algorithms for molecular dynamics simulations on commodity clusters. proceedings of the ACM/IEEE conference on supercomputing (sc06), Tampa, Florida 2006; 11-17.
35. Kaminski GA: Evaluation and reparametrization of the opls-aa force field for proteins *via* comparison with accurate quantum chemical calculations on peptides. J Phys Chem B 2001; 105(28): 6474-87.
36. Tian X, Xu Z, Li Z, Ma Y, Lian S, Guo X, Hu P, Gao Y and Huang C: Pharmacokinetics of mangiferin and its metabolite-norathyriol, Part 2: Influence of UGT, CYP450, P-gp and enterobacteria and the potential interaction in Rhizoma Anemarrhenae decoction with timosaponin B2 as the major contributor. BioFactors 2016; doi: 10.1002/biof.1290.

How to cite this article:
Manikyam HK: Study of mangiferin isolated from leaves of *Mangifera indica* on myeloid leukemia along with different human cancer cell lines. Int J Pharm Sci & Res 2019; 10(12): 5545-52. doi: 10.13040/IJPSR.0975-8232.10(12).5545-52.

All © 2013 are reserved by the International Journal of Pharmaceutical Sciences and Research. This Journal licensed under a Creative Commons Attribution-NonCommercial-ShareAlike 3.0 Unported License.

This article can be downloaded to **Android OS** based mobile. Scan QR Code using Code/Bar Scanner from your mobile. (Scanners are available on Google Playstore)